5th Joint International Symposium on Deformation Monitoring (JISDM), 20-22 June 2022, Valencia, Spain
DOI: http://doi.org/10.4995/JISDM2022.2022.13635

Two multi-wavelength interferometers for large-scale surveying

Anni Sauthoff[1], Paul Köchert[1], Günther Prellinger[1], Tobias Meyer[1], Frank Pilarski[1], Stephanie Weinrich[1], Frank Schmaljohann[1], Joffray Guillory[2], Daniel Truong[2], Jakob Silbermann[3], Ulla Kallio[4], Jorma Jokela[4], Florian Pollinger[1]

[1] Physikalisch-Technische Bundesanstalt (PTB), Bundesallee 100, 38116 Braunschweig, Germany, (anni.sauthoff@ptb.de; paul.koechert@ptb.de; guenther.prellinger@ptb.de; tobias.meyer@ptb.de; frank.pilarski@ptb.de; stephanie.weinrich@ptb.de; frank.schmaljohann@ptb.de; florian.pollinger@ptb.de)
[2] Conservatoire National des Arts et Métiers (Cnam), Laboratoire commun de métrologie LNE-Cnam, 1 rue Gaston Boissier, 75015 Paris, France, (joffray.guillory@cnam.fr; daniel.truong@cnam.fr)
[3] Bernhard Halle Nachfl. GmbH, Hubertusstr. 10, 12163 Berlin, Germany, (jakob.silbermann@b-halle.de)
[4] Finnish Geospatial Research Institute, National Land Survey of Finland, Geodeetinrinne 2, 02430 Masala, Finland, (ulla.kallio@nls.fi; jorma.jokela@nls.fi)

Key words: *two-colour refractivity compensation; multi-wavelength interferometry; multilateration; system design; long range measurement*

ABSTRACT

Deformation monitoring requires the detection of smallest changes, always at the limits of technical feasibility. Trying to push these limits further, we have realised two terrestrial ranging instruments: a long-range 1D electro-optic distance meter and a 3D multilateration-capable sensor system of 50 m range. The former one is intended as primary standard for the calibration of geodetic instrumentation with low uncertainty to the SI definition of the metre. The latter one is intended for monitoring larger monuments like VLBI antennas. In this contribution, we describe the technical challenges and our solutions for such instrumentation. We use the two-colour method for inline refractive index compensation. As common optical source, we developed a versatile multi-wavelength generator based on two Nd:YAG lasers stabilised by a phase-locked loop realised by Field Programmable Gate Arrays (FPGA). The 1D interferometer uses custom-designed achromatic optics and a mechanical frame optimised for form stability under field conditions. The phase demodulation system allows for maximum range flexibility from several meters up to several kilometres. The base ranging unit of the 3D multilateration system adheres to a different demodulation technique, which allows a relatively simple interferometer head design. This approach requires a sophisticated source modulation scheme limiting the applicability to distances over 15 m up to approximately 50 m in our case.

I. INTRODUCTION

Commercial electronic distance meters (EDM) are mainly based on amplitude modulation (Köhler, 2012). In the last years several research projects have shown that this concept has not achieved its resolution limits yet. Modern photonics and electronics enable working with radio frequencies of several Gigahertz (Guillory *et al.*, 2016). Standard deviations below 30 µm over 5.4 km have been demonstrated (Guillory *et al.*, 2019). High modulation frequencies can also be generated making use of modern optical sources. Intermode beats of optical frequency combs make modulation frequencies of several tens to hundred Gigahertz possible (Minoshima and Matsumoto, 2000). Millimetric accuracy up to 600 m under field conditions have been demonstrated with this technique (Pollinger *et al.*, 2012). Absolute interferometry can be an alternative for highly precise distance measurements in surveying. This technique mainly developed for precision engineering relies on one or more optical interference measurements and uses the optical wavelength as a very sensitive scale for the measurement. Unlike classical interferometry, the absolute distance is not acquired by a continuous displacement measurement in which the reflector is moved relatively over the distance to be measured, but by a sophisticated measurement strategy like frequency sweeping interferometry (FSI, *e.g.* Meiners-Hagen *et al.*, 2009) or fixed synthetic multi-wavelength interferometry. Conceptual studies have shown the enormous potential of this technique driven by optical frequency combs (van den Berg *et al.*, 2012; Coddington *et al.*, 2009) in the laboratory, but also sub-millimetric accuracy over 1.2 km measurement range in free space has already been successfully demonstrated (Wu *et al.*, 2017).

The achievable uncertainty of any optical measurement in surveying, however, is limited by the fact that the measurement is performed in air and the index of refraction needs to be properly considered. The inhomogeneity of the index of refraction parallel to the optical beam propagation direction limits the achievable uncertainty of the optical distance measurement. Elaborate sensor networks can mitigate

this problem, *e.g.* at reference baselines (Pollinger *et al*., 2012; Neyezhmakov *et al*., 2020). Ideally, however, the effective index of refraction is measured in the same volume as the optical beam. There are multiple approaches, based, *e.g.*, on a measurement of the speed of sound (Pisani *et al*., 2018), or on spectroscopy (Tomberg *et al*., 2017). We pursue the two-colour method which was originally introduced in 1965 by Bender and Owens for surveying purposes. Initial instrumental realisations (Earnshaw and Owens, 1967) climaxed in the famous commercial two-colour terrameter (Hugget and Slater, 1975; Hugget, 1981). Since knowledge of the index of refraction limits the achievable uncertainty in large-scale distance measurements today, interest in this technology has recently considerably increased again. Meiners-Hagen and Abou-Zeid provided an extended model for humid air in 2008. The two-colour method is especially interesting for broadband optical sources like optical frequency combs as they provide the necessary spectrum for this measurement technology (Minoshima and Matsumoto, 2000; Salido-Monzú and Wieser, 2018). Stabilities of 10^{-11} over 500 s were demonstrated for distance measurements in the laboratory (Wu *et al*., 2013). We demonstrated application of the two-colour method to long distance measurements (Meiners-Hagen *et al*., 2015; Meiners-Hagen *et al*., 2017) and to measurements over several tens of metres in industrial environments (Meiners-Hagen *et al*., 2016). In this contribution, we describe two multi-wavelength interferometers developed for two different application scenarios in large-scale surveying. The TeleYAG-II interferometer is designed for the low-uncertainty, SI-traceable measurement of reference baselines with a range of up to 5 km. This relatively long range is relevant for the ground-based SI-traceable verification of space-geodetic techniques like Satellite-Laser-Ranging (SLR) or global navigation satellite systems (GNSS). The Absolute3D interferometer, on the other hand, is developed as an absolute interferometer for a range of several tens of meters. It is intended for multilateration-monitoring of larger critical structures like VLBI antennas. Although their fundamental physical working principles are nearly identical, the different use cases require two substantially different technical realisations. In the paper, we briefly review the fundamentals of multi-wavelength interferometry and two-colour refractive index compensation and describe the challenges for the technical and field-capable realisation of these ideas (Section II). We introduce the multi-wavelength source we developed for both systems (Section III) and then describe the two interferometer systems with an emphasis on their response to the application challenges (Sections IV and V).

II. METHOD

A. *Two-colour method*

The refractive index of air depends on the vacuum wavelengths λ, and the thermodynamic properties ambient pressure *p,* temperature *T*, water vapor pressure p_w and carbon dioxide contents *x* (*e.g.* Bönsch and Potulski, 1998). The basic concept of the two-colour method is based on the fact that the dependencies on wavelength and environmental parameters separate naturally in the typical functional model of the form (Eq. 1):

$$n(\lambda, T, p, x, p_w) - 1 = K(\lambda) \cdot D(T, p, x) - p_w g(\lambda) \qquad (1)$$

with the functionals *K(λ)* representing the dispersion term*, D(T, p, x)* the density term, and *g(λ)* the humidity term (Meiners-Hagen *et al*., 2017). If the optical path lengths d_1 and d_2 of an identical geometric distance are measured with two different wavelengths (λ_1, λ_2), the geometric length l can be expressed by the respective vacuum wavelengths and the corresponding refractive index (Eq. 2):

$$l\, n_1 = d_1; \quad l\, n_2 = d_2. \qquad (2)$$

Inserting Equation 1 leads to a system of equations which can be solved for the geometric length by (Eq. 3):

$$l = \frac{K_1 d_2 - K_2 d_1}{K_1 - K_2 + p_w\left(g_1 K_2 - g_2 K_1\right)}. \qquad (3)$$

The geometric length can hence be measured without explicitly detecting most of the ambient conditions. Nevertheless, a very accurate measurement of the raw optical path lengths d_1 and d_2 (*i.e.* the observed distances uncorrected for the index of refraction) is required to achieve a sufficient uncertainty of the geometric length.

B. *Multi-wavelength interferometry*

An ordinary counting interferometer is based on interference fringe counting while moving one reflector. When the integer order is lost, *e.g.*, due to a fast and discontinuous movement, only the fractional order of interference is obtained (phase/2π). The range of unambiguity can be enlarged by using more than one wavelength. The difference between two interferometric phases ϕ_1, ϕ_2 of two optical wavelengths can be interpreted as a differential phase (Eq. 4):

$$\phi = \phi_2 - \phi_1 \qquad (4)$$

which can be interpreted as interference phase of a virtual synthetic wavelength (Eq. 5):

$$\Lambda = \frac{\lambda_1 \lambda_2}{\lambda_1 - \lambda_2}. \quad (5)$$

The synthetic wavelength Λ is always longer than the two optical vacuum wavelengths λ_1 and λ_2. In consequence, any uncertainty of the phase measurement is multiplied by the synthetic wavelength, increasing the actual length uncertainty by a factor of Λ/λ in comparison to a classic interference measurement. Long synthetics hence imply high uncertainties. But the range of non-ambiguity is limited to half of the synthetic wavelength, comparable to the limitation of the 'scale' given by the modulation frequencies in classical EDM. Instead of working with long synthetics, the remaining ambiguity can be resolved using FSI. The interferometer phase for a given light frequency ν is generally expressed by (Eq. 6):

$$\phi = \frac{4\pi\nu}{c} nl \quad (6)$$

with c representing the vacuum speed of light. For the variable synthetic wavelengths approach the laser frequency ν is tuned by $\Delta\nu$. If the synthetic phase change $\Delta\Phi$ is simultaneously tracked, the absolute geometric length l can be calculated by (Eq. 7):

$$\mathrm{l} = \frac{c}{4\pi n_g} \frac{\Delta\Phi}{\Delta\nu}. \quad (7)$$

It should be noted that the target is required to stand reasonably still during such a frequency sweep for the measurement to work.

C. *Technical challenges*

Although the fundamentals of dispersion-compensating multi-wavelength interferometry may seem straightforward, its implementation for geodetic purposes poses multiple technical challenges. First, the provided laser source must emit light of a high degree of coherence. Furthermore, the prerequisite for multi-wavelength interferometry is a perfect geometrical superposition of all optical beams. Otherwise, a difference in length measurement would not only attribute to the refractive index, but also to a cosine error between the different beam paths. Classical free-space beam superposition is instable, hard to achieve and to control outside the lab. A more elegant and robust way is to combine the beam paths in a photonic crystal fibre (PCF) (Liu *et al.*, 2020). The PCF automatically ensures a perfect superposition of the optical beams and reduces the number of mirrors and therefore the time for readjustments. The emitted beam size by a PCF, however, strongly depends on the wavelength. This needs to be considered in the optics design. Moreover, all optics need to be carefully achromatically designed because the wavelengths used for dispersion compensation are usually strongly spectrally separated. Finally, optical phases must be detected for every wavelength used and correctly assigned. This implies that the phases or respectively colours can be separated before detection. For the spectrally well-separated fundamental working wavelengths, like 532 nm and 1064 nm, this can be achieved by standard optical means like dichroitic mirrors. But for separating the two wavelengths used for the fixed synthetic wavelengths (differing in our case only by 20 GHz or about 0.1 nm) alternative electronic demodulation schemes are needed.

III. Multi-wavelength source

One key requirement for the realisation of a geodetic multi-wavelength measurement is hence an optical source providing light at multiple well-defined wavelengths and sufficient coherence. Furthermore, a demodulation scheme needs to be implemented. For this purpose, we developed a versatile multi-wavelength source consisting of Nd:YAG lasers (model: Innolight Prometheus 20NE) and a modulation technique that varies depending on the application scenario the respective interferometer.

The Nd:YAG lasers provide wavelengths at 1064 nm and 532 nm and an optical power of each laser of 1 W and 20 mW, respectively. The 532 nm wavelength is generated by second harmonic generation (SHG) and is intrinsically phase-stable to the 1064 nm wavelength (Wynands *et al.*, 1995). Their energy efficiency, size, lifetime, robustness, and intrinsic noise levels, render diode-pumped solid-state lasers like Nd:YAG lasers ideal for the use in multi-wavelength interferometry. The coherence length of Nd:YAG ring oscillators has been subject of investigation in prior research (Sorin *et al.*, 1990): with self-interference techniques using a delay fibre line of 100 km, coherence was still observable. Czarske *et al.* estimated in 1995 that Nd:YAG oscillators had linewidth properties to measure distances of more than 1000 km.

The design of the multi-wavelength source should be as simple as possible to cope with the uncertainties during field operation. Therefore, in contrast to numerous scientific works in the field of laser stabilisation, no measures were taken to protect the laser sources from disturbing sources. Multiple wavelengths were generated in three ways: by offset locking of the fundamental wavelengths at a beat frequency of 20 GHz using an optical phase-locked loop (OPLL), by shifting the laser frequency using acousto-optic modulators (AOMs) and by modulating the wavelength using piezo transducer (PZT).

A. *OPLL offset lock*

The setup for the OPLL is summarized in Figure 1a. Both independent laser oscillators, the so-called master and slave laser, are phase-locked using their 1064 nm outputs by the well-known offset-locking technique. The heterodyned optical signal is converted into a

microwave signal using a fibre-coupled photo detector (New Focus 1414, 25 GHz bandwidth). To precisely tune the frequency offset between both phase-locked lasers, a super high frequency (SHF) synthesizer (R&S SMA-100B) with low noise characteristics (R&S SMAB-B710; single-sideband (SSB) phase noise, typical -111 dBc at 1 kHz offset), is employed as an offset stage to down convert the 20 GHz beat signal with a mixer to an intermediate frequency of 62.5 MHz. The down-mixed signal is then sampled with a sample rate of 250 MSPS by a 14 bit analogue-to-digital-converter (ADC, ADS62P49) equipped on a transceiver board (NI-5782), which is connected to an FPGA-based controller (NI-7935R, Kintex-7-410T). The FPGA executes an I/Q demodulation algorithm to extract the phase information from the data stream with a low latency of about 1 µs. The data processing is based on a 256 tap FIR filter with a bandwidth between 125 kHz and 10 MHz, which is adjustable to meet the boundary conditions of our two interferometer systems. We choose a minimum bandwidth of 125 kHz for TeleYAG-II measurements to optimally reject disturbances, while the bandwidth is increased to more than 4 MHz for the Absolute3D system to tolerate the frequency deviation of the modulated signals. Finally, the phase information is used to process two output signals with a cascaded PID control method. While a 16 bit fast control output (DAC5682Z, SFDR: 77 dB) is fed to the PZT actuator, a slower 20 bit (AD5791, SFDR: 100 dB) is used to precisely control the crystal temperature. To determine the wavelength instability of the offset-locked laser system, we recorded the 62.5 MHz waveform at the maximum acquisition rate of 250 MSPS over a measurement time of 4 s (Figure 1b). The 2 GB data sampled by our controller were post processed to estimate the power spectral density (method according to Welch 1967 50% overlap). It turned out that without any averaging a stability of about 2 kHz FWHM can be achieved for the 20.0625 GHz beat node, which is equivalent to a relative value of $1 \cdot 10^{-7}$. This corresponds to an error of ± 0.75 nm for a single 15 mm synthetic wavelength at 1064 nm for our multi-wavelength interferometers. For fixed synthetic wavelengths interferometry, we typically choose an offset frequency of 20 GHz, generating synthetic wavelengths of 14.94 mm at 1064 nm and of 7.47 mm at 532 nm. By varying the synthesizer frequency, the frequency of the slave laser can be continuously tuned in this scheme, enabling a 'super-heterodyning' detection mode (Dändliker *et al.*, 1988).

B. *Modulation techniques*

Figure 2 summarises the different modulation techniques used for phase retrieval by the two interferometers. The TeleYAG-II interferometer uses a classical heterodyne demodulation scheme. This enables the separation of optical phases of closely adjacent optical wavelengths by lock-in techniques, Thus, a minimal set of photo detectors is sufficient for detection (Köchert *et al.*, 2012; Yang *et al.*, 2015). For the TeleYAG-II system, we use acousto-optic modulators (AOMs) to generate eight different carrier frequencies. In addition to the relatively short synthetic wavelengths generated by the OPLL, the wavelength shift by the AOMs is also used to realise two synthetic wavelengths of 1.486 m at 1064 nm which are continuously emitted in parallel. In contrast to our previous work (Meiners-Hagen *et al.*, 2015), we use eight fibre-coupled AOMs (3x VIS, 5x NIR) to generate the carriers and to enhance the robustness of the overall system, improving field capability. After passing through the interferometer optics, the light is subject of interference and can be detected by two photo receivers for each colour which convert the optical to a voltage signal. The voltage signals contain the carrier frequencies and are fed to an in-house developed phase meter (ADC board NI-5762, 75.5-dB SNR). It is capable of extracting the phase information for each carrier. In the post-processing step, the phase information is used to unfold the multiple wavelengths to determine the absolute value of the distance measurement.

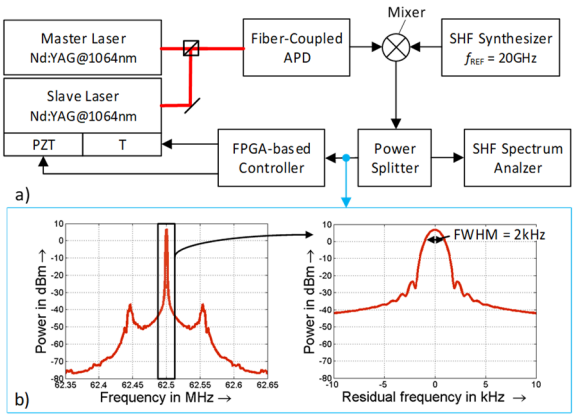

Figure 1. (a) Simplified scheme of the OPLL for locking both lasers with a frequency offset of 20 GHz. (b) Spectrum of intermediate frequency to distinguish the Full Width Half Maximum (FWHM). (T – Temperature, PZT – Piezo Transducer, SHF – Super High Frequency, APD – Avalanche Photo Diode).

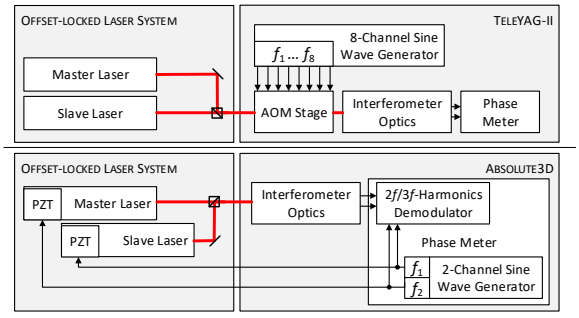

Figure 2. Scheme of the different modulation techniques.

The Absolute3D interferometer makes use of a sinusoidal modulation technique (Suzuki, 1989), enabling a more compact measurement head. The wavelengths of the master and slave lasers are phase

modulated by using the integrated piezo transducer with two independent carrier frequencies in the range of 20 kHz to 30 kHz and modulation widths of about 2.3 MHz at 1064 nm. The modulation signals are generated using the same FPGA-based electronics used to record the interference signals. The optical signals are converted into electrical signals, which are then decomposed on the FPGA in real time with respect to its second ($2f_1$, $2f_2$) and third order ($3f_1$, $3f_2$) harmonic components according to Sudarshanam and Srinivasan (1989). From the relationship between signals $2f_1/3f_1$ and $2f_2/3f_2$, the phase information corresponding to the absolute distance can be determined.

IV. The TeleYAG-II interferometer

The TeleYAG-II interferometer follows the heterodyne approach used for the original TeleYAG interferometer (Meiners-Hagen *et al*., 2015). However, we use PCFs to superpose the 532 nm and 1064 nm beams. In consequence, all optical components need to be achromatic and anti-reflection coated for both wavelengths. The system is supposed to reliably work outside. The complex optical setup and the long optical paths in the system imply a large sensitivity to thermally induced drifts. In our case, even small drifts are fatal for the measurement result as any uncertainty in the interferometric measurement is highly unfavourably scaled up due to the multi-wavelength measurement approach. We therefore very carefully designed the interferometer head for mechanical stability, using mainly invar as material with a low coefficient of thermal expansion (CTE) (Pilarski *et al*., 2021). To monitor remaining drifts, we introduce a retractable reference mirror in the measurement path. The targeted range of 5 km is a particular challenge for the imaging optics. The two main colours of the system, 532 and 1064 nm, pass the same optics on the interferometer head. Any chromatic error would fatally propagate. In Figure 3a, the custom-designed achromatic telescope lenses of the expansion optics are depicted. The ocular consists of a lens doublet, the objective of a lens triplet. The optics design for this long-range two-colour system is non-trivial for two reasons. In general, a simple linear optics approximation cannot be used to describe the beam propagation for a confined laser beam given the inevitable extreme spot size to propagation distance ratio for distances over several hundreds of meters. We must consider that the beams do not propagate with planar wavefronts, but as Gaussian beams. In this context, the most critical aspect is the fact that Gaussian beams propagate in curved wave fronts. The most unfavourable consequence thereof is the fact, that Gaussian beams cannot be collimated in the sense of linear optics, but continuously change their beam waist over their propagation distance. This effect is usually mitigated by choosing larger initial beam waists. But in our case, even when choosing an aperture of 119 mm, after propagation over several thousands of metres, the beam waist considerably enlarges so that clipping at the aperture cannot be completely avoided (compare beam expansion between point B and C in Figure 3b). This effect is worsened by a second particularity of our optics design. As mentioned, we use a PCF to superpose the infrared and the green light. The price to pay for this perfect concentric overlap, however, is the fact that the beams emitted by the fibre vary in their spot size, depending on the optical wavelength. For the 532/1064 nm pair, the beam size almost doubles for the longer wavelength (dashed lines A in Figure 3c). Our optical system is designed so that up to approximately 1000 m measurement distance, the returning wavefront (labelled D in Figure 3c) matches almost perfectly the reference wave front in the interferometer head (A in Figure 3c). For longer distances, this match can only be imperfectly assured, possibly requiring a length-dependent correction factor. Furthermore, to realise the large beam expansion, the distance between ocular and objective lens amounts to 486 mm. To limit the extensions of the whole instrument, we chose a sandwich structure with interferometer and beam expansion being positioned on different levels (see Figure 3a). We also want to note that, like in every telescope, this distance is highly critical for the imaging properties of the expansion optics. For the TeleYAG-II system, the ocular position Δz (*cf.* Figure 3a) should not deviate more than 100 µm from the optimum lens position, given by the sum of the lenses' focal lengths according to the simulation. Bigger deviations considerably deteriorate the beam collimation. As consequence, the sharp increase in beam diameter visible in Figure 3b moves to shorter and shorter distances, which quickly significantly reduces the application range. Therefore, a fine-tuneable solid-state joint was designed for ocular positioning. The absolute distance is also fixed by the low CTE material of the interferometer frame.

Figure 4 depicts a typical observation indoors over a range of approximately 26 m. The data have been recorded at a rate of 1024 data points per second for one minute. For the analysis, we require that the interference contrast in all six interferometers (two at 532 nm, four at 1064 nm) is between 25 and 99 % of the maximum of each channel. Only 52.9 % of all data sets pass this filtering process. We depict the measurement results using the high-resolution data with the shortest synthetic wavelengths at 1064 nm and 532 nm. For the power-filtered raw data, we obtain a standard deviation of 82 µm at 1064 nm, 57 µm at 532 nm. Averaging over 1024 data points, the standard deviation at 532 nm reduces to 11 µm, at 1064 nm to 53 µm only. The bad scaling properties of the 1064 nm result indicates a more fundamental problem. Currently, we revise the optical setup to facilitate the alignment of the infrared beams, hoping to improve the performance. It should also be noted that preliminary results over distances over 800 m outdoors show standard deviations of

similar magnitude, indicating that the optical system manages to preserve the fundamental performance over such long distances as desired.

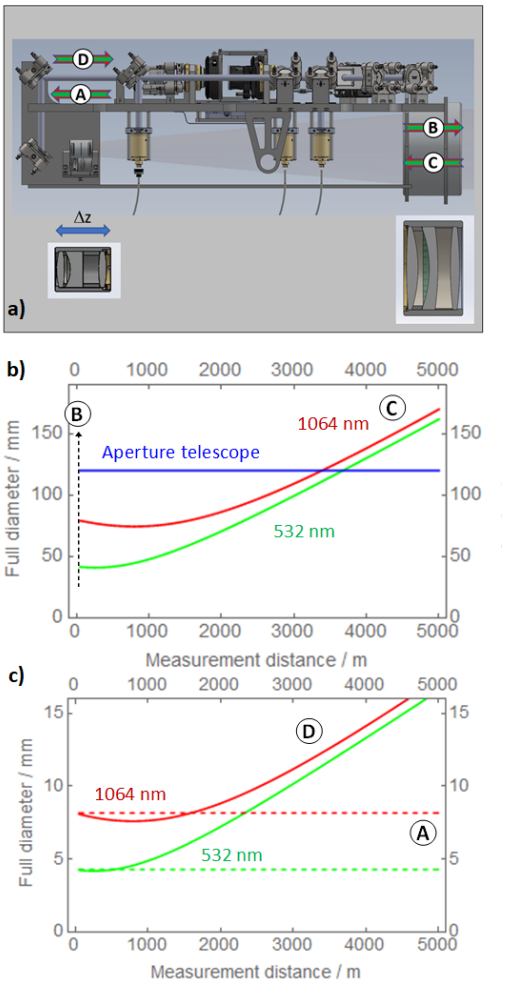

Figure 3. Beam expansion optics of the TeleYAG-II interferometer: a) Beam path in the expansion optics and cut through the achromatic telescope lenses. b) Calculated full beam diameter (2ω beam waist) before re-entering the telescope. c) Matching of the full beam diameters (2ω beam waist) of returned and emitted beam in the interferometer itself. The figures b) and c) are based on a configuration with Δz = 20 µm.

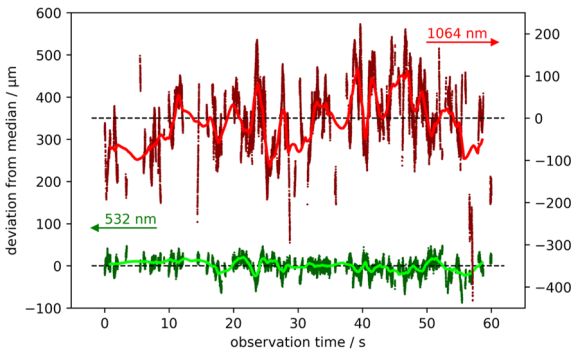

Figure 4. Typical observation data with the TeleYAG-II system over 26 m indoors. The data shows the deviation from the median value for the position data obtained from the synthetic wavelengths at 532 nm and 1064 nm. The scattered data show the power-filtered raw data, the lines indicate a moving average over 1024 data points.

V. The Absolute 3D interferometer

The Absolute3D system targets a more flexible and better affordable interferometer design for shorter ranges. Thus, multiple interferometer heads can be more easily constructed. The intended applications comprise multilateration measurements requiring four heads or the intrinsic measurement of vertical temperature gradients (Röse *et al.*, 2020). Compared to the TeleYAG-II system we reduced the optical setup to a minimum complexity level at the cost of the rather complex phase detection scheme based on sinusoidal modulation. For the interferometer set up the compact Michelson design was chosen. The reduced number of optical elements in the structure means that the system can be easily readjusted in case of changes due to vibrations or environmental changes. The interferometer platforms are mounted on gimbal systems (Zaber: X-G-RST300) which enable horizontal and lateral movements (see Figure 5). The interferometer itself and its source are decoupled but connected by a single PCF only, while the TeleYAG-II system requires two PCFs. Auxiliary instrumentation needed for signal generation and analysis can be stowed in a nearby trailer.

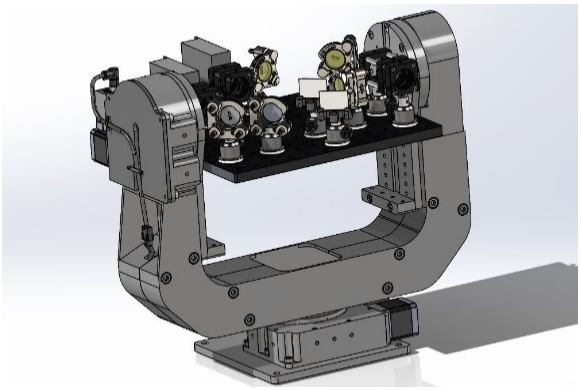

Figure 5. 3D Sketch Absolut3D on Gimbal System (model: Zaber X-G-RST300).

The length measurement consists of two partial measurements. Two Nd:YAG lasers are being used. Their laser frequency is sinusoidally modulated to enable the 2f/3f detection scheme. In static operation mode, their frequency offset is fixed to 20.0625 GHz, corresponding to synthetic wavelengths of Λ_1 =14.89 mm at 1064 nm and of Λ_2 = 7.48 mm at 532 nm. The flexible application scenario requires a truly absolute measurement. We realise a variable synthetic interferometry measurement within the same setup by sweeping the frequency of the slave laser. To guarantee the best optical superposition of all four laser paths, we couple them into a PCF. We use two beam splitters to superpose the two 1064 nm as well as the two 532 nm beams first. A second beam splitter in the infrared path splits the already superposed beam paths and provides the light necessary for the laser stabilization. We use a dichroic mirror to superimpose these two beams. Usually, a coupling rate of about 70%

can be achieved for each beam path. The optical system encounters similar problems regarding beam expansion and chromaticity errors as the TeleYAG-II interfero meter. But since the range is limited to 50 m, a single custom-designed achromatic triplet lens collimating the beams of the PCF is sufficient. The system works with a full beam diameter of 12 mm at 1064 nm and 6 mm at 532 nm. After interference of measurement and reference beams, a dichroitic mirror separates the infrared from the visual beams. They are subsequently detected in a separate photoreceiver (Femto: HCA-S-200M-Si & HCA-S-200M-IN). All four phases of the interferometric signal are then derived by the 2f/3f lock-in technique.

In Figure 6, a typical indoor measurement of a fixed position at approx. 26 m is depicted. A sweep of 1 GHz at 1064 nm (corresponding to 2 GHz at 532 nm) with one laser was performed for a variable synthetic wavelength measurement to determine a pre-value of the geometric distance from the corresponding absolute phase change (see inset of Figure 6). We then use the phase information of the fixed synthetic wavelength measurement performed on plateau 1 (P1 in Figure 6) to refine this pre-value. This leads to a total optical distance of d_1 = 26.017858 m for the 532 nm measurement and of d_2 = 26.017520 m for the 1064 nm measurement. Using Equation 3 with a water vapor pressure p_W of 1188 Pa, we can now directly calculate the geometric length to l = 26.0107 m. The standard deviation of the acquired geometric length amounts to 1.8 mm. Theory predicts the standard deviation of the refractivity-compensated result to scale by a factor of 21 in comparison to standard deviation of the underlying observation at 532 nm. The raw 1064 nm data shows a standard deviation of 119 µm, the raw 532 nm data of 42 µm which reduce to 109 µm and 40 µm for 1024 points (1 second) averaging (*cf.* Figure 6). As expected, both signals largely show a common-mode behaviour due to the environmental influences. These are then compensated by the application of Equation 3. Thus, we would expect a standard deviation of the compensated result in the order of 0.8 mm. Nevertheless, inconsistencies like subtle differences in the drift behaviour indicate additional unresolved error sources. We currently investigate probable origins. We work, *e.g.*, on the enhanced compensation of nonlinear effects, to which sinusoidal modulation is notoriously sensitive. Ultimately, we target a measurement uncertainty of a few tenths of a millimetre for the refractivity-compensated length.

VI. Conclusions

In this paper we discuss two multi-wavelength interferometers to achieve high accuracy measurements for different geodetic applications: one for 1D measurements distances up to 5 km, one for 3D measurements within a measurement volume of approximately 50 m. Both systems rely on a complex versatile multi-wavelength optical source based on two Nd:YAG lasers. Their optical design and phase demodulation varies to match their use cases. In Table 1, we summarise key technical features of both systems. So far, they have not achieved the full targeted measurement capability, but show similar standard deviations and first meaningful intrinsically refractivity-compensated distance measurements could be demonstrated over relevant longer distances. In future, the systems will be further optimised and applied to geodetic measurement challenges.

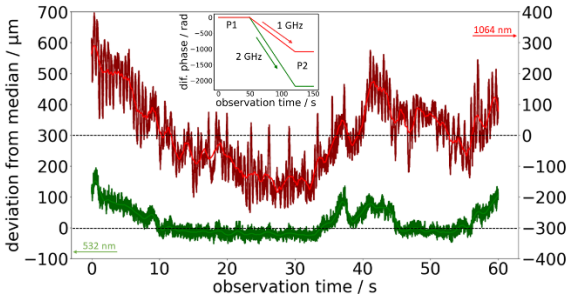

Figure 6. Typical observation data with the Absolute3D system over 26 m indoors. The data shows the deviation from the median value for the position data obtained from the synthetic wavelengths at 532 and 1064 nm. The lines indicate a moving average over 1024 data points. The inset depicts the phase hub while tuning one laser to determine the pre-value.

Table 1. Key features of the two interferometers

TeleYAG-II	Absolute3D
PCF architecture for broadband beam superposition Based on two Nd:YAG laser sources	
Frequency modulation by AOMs	Sinusoidal phase modulation by laser resonators
4 achromats	1 achromat per head
Complex optical setup (Sandwich structure)	Simple optical setup (Michelson Interferometer)
Range up to 5 km	Range 15 m to 50 m
1 head	4 optical heads
Weight ~50 kg	Weight ~20 kg (each)

VII. Acknowledgements

This project 18SIB01 GeoMetre has received funding from the EMPIR programme co-financed by the Participating States and from the European Union's Horizon 2020 research and innovation programme. We would like to thank P. Knigge, D. Fiala, M. Wedde, and M. Peglow for technical assistance.

References

Bender, P. L., and Owens, J. C. (1965) Correction of optical distance measurements for the fluctuating atmospheric index of refraction. *J. Geophys. Res.* 70, pp. 2461–2.

van den Berg, S., Persijn, S., Kok, G., Zeitouny, M., and Bhattacharya, N. (2012) Many-wavelength interferometry

with thousands of lasers for absolute distance measurement. *Phys. Rev. Lett.* 108, 183901 (5 pp.).

Bönsch, G., Potulski, E. (1998), Measurement of the refractive index of air and comparison with modified Edlén's formulae. *Metrologia* 35, pp. 133-9.

Coddington, I., Swann, W. C., Nenadovic, L. and Newbury, N. R. (2009) Rapid and precise absolute distance measurements at long range. *Nat. Photonics* 3, pp. 351–6.

Czarske, J. W., Phillipps, R., and Freitag, I. (1995) Spectral properties of diode-pumped non-planar monolithic Nd:YAG ring lasers. *Appl. Phys. B* 61, pp. 243-8.

Dändliker, R., Thalmann, R., and Prongue, D. (1988) Two-wavelength laser interferometry using superheterodyne detection. *Opt. Lett.* 13, 339–41.

Earnshaw, K. B., and Owens, J. C. (1967) Dual wavelength optical distance measuring instrument, which corrects for air density. *IEEE J. Quantum Electron*. 3, pp. 544–50.

Guillory, J., Šmid, R., Garcia-Marquez, J., Truong, D. Alexandre, C., and Wallerand, J.-P. (2016) High resolution kilometric range optical telemetry in air by radio frequency phase measurement. *Rev. Sci. Instr*. 87, 075105 (6 pp.).

Guillory, J., Teyssendier de la Serve, M., Truong, D., Alexandre, C. and J.-P. Wallerand (2019) Uncertainty assessment of optical distance measurements at micrometer level accuracy for long-range applications. *IEEE Trans. Instrum. Meas*. 68, pp. 2260–2267.

Hugget, G.R. and Slater, L.E. (1975) Precison electromagnetic distance measuring instrument for determining secular strain and fault movement. *Tectonophysics* 29, pp. 19-27.

Huggett, G.R. (1981) Two-color terrameter*. Tectonophysics* 71, pp. 29–39.

Köchert, P., Flügge, J., Weichert, C., Köning, R., and Manske, E. (2012) Phase measurement of various commercial heterodyne He-Ne-laser interferometers with stability in the picometer regime. *Meas. Sci. Technol.* 23, 074005 (6 pp.).

Köhler, M. (2012) Distanzmessverfahren elektrooptischer Tachymeter – Stand der Trimble Technik. *avn* 119, pp. 291-304.

Liu, Y., Röse, A., Prellinger, G., Köchert, P., Jigui, Z., and Polliner, F. (2020) Combining Harmonic Laser Beams by Fiber Components for Refractivity-Compensating Two-Color Interferometry. *J. Light. Technol.* 38, pp. 1945-52.

Meiners-Hagen, K., and Abou-Zeid, A. (2008) Refractive index determination in length measurement by two-colour interferometry. *Meas. Sci. Technol.* 19, 084004 (5 pp.).

Meiners-Hagen, K., Schödel, R., Pollinger, F., and Abou-Zeid, A. (2009), Multi-Wavelength Interferometry for Length Measurements Using Diode Lasers. *Meas. Sci. Rev.* 9, pp. 16-26.

Meiners-Hagen, K., Bosnjakovic, A., Köchert, P., and Pollinger, F. (2015) Air index compensated interferometer as a prospective novel primary standard for baseline calibrations. *Meas. Sci. Technol.* 26, 084002 (8 pp.).

Meiners-Hagen, K., Meyer, T., Prellinger, G., Pöschel, W., Dontsov, D., and Pollinger, F. (2016). Overcoming the refractivity limit in manufacturing environment. *Opt. Express* 24, pp. 24092–104.

Meiners-Hagen, K., Meyer, T., Mildner, J., and Pollinger, F. (2017) SI-traceable absolute distance measurement over more than 800 meters with sub-nanometer interferometry by two-color inline refractivity compensation. *Appl. Phys. Lett*. 111, 191104 (5 pp.).

Minoshima, K., and Matsumoto, H. (2000) High-accuracy measurement of 240-m distance in an optical tunnel by use of a compact femtosecond laser. *Appl. Opt.* 39 5512–7.

Neyezhmakov, P., Panasenko, T., Prokopov, A., Skliarov, V., and Trevoho, I. (2020). Comparative analysis of quadrature formulas for the mean integral refractive index of air in high-precision ranging. *Modern achievements of geodesic science and industry* 39, pp. 69–73.

Pilarski, F., Schmaljohann, F., Weinrich, S., Huismann, J., Truong, D., Meyer, T., Köchert, P., Schödel, T., and Pollinger, F. (2021). Design and manufacture of a reference interferometer for long-range distance metrology. In: Proc. Euspen's 21st International Conference & Exhibition, Virtual Conference, 7-10, June, pp. 511–512.

Pisani, M., Astrua, M., and Zucco, M. (2018). An acoustic thermometer for air refractive index estimation in long distance interferometric measurements. *Metrologia* 55, pp. 67–74.

Pollinger, F., Meyer, T., Beyer, J., Doloca. N. R., Schellin, W., Niemeier, W., Jokela, J., Häkli, P., Abou-Zeid, A. and Meiners-Hagen, K. (2012) The upgraded PTB 600 m baseline: a high-accuracy reference for the calibration and the development of long distance measurement devices. *Meas. Sci. Technol.* 23, 094018 (11 pp.).

Röse, A., Liu, Y., Köchert, P., Prellinger, G., Manske, E., and Pollinger, F. (2020) Modulation-based long-range interferometry as basis for an optical two-color temperature sensor. In: Conference Proceedings - 20th International Conference & Exhibition, Geneva, CH, June 2020.

Salido-Monzú, D., and Wieser, A. (2018) Simultaneous distance measurement at multiple wavelengths using the intermode beats from a femtosecond laser coherent supercontinuum. *Opt. Eng.* 57, 044107 (10 pp.).

Sorin, W.V., Donald, D.K., Newton, S.A., and Nazarathy, M. (1990) Coherent FMCW reflectometry using a temperature tuned Nd:YAG ring laser. *IEEE Phot. Technol. Lett.* 2, pp. 902–4.

Sudarshanam, V.S., and Srinivasan, K. (1989)Linear readout of dynamic phase change in a fiber optic homodyne interferometer, *Opt. Lett.* 14, pp. 140–2.

Suzuki, T., Sasaki, O., Higuchi, K. and Maruyama, T. (1989) Real time displacement measurement in sinusoidal phase modulating interferometry, *Appl. Opt*. 28, pp. 5270–4.

Tomberg, T., Fordell, T., Jokela, J., Merimaa, M., and Hieta, T. (2017) Spectroscopic thermometry for long-distance surveying. *Appl. Opt.* 56, pp. 239–46.

Welch, D. (1967) The use of fast Fourier transform for the estimation of power spectra *IEEE Trans. Audio Electroacoustics* 15, pp. 70–73.

Wu, G., Takahashi, M., Arai, K., Inaba, H., and Minoshima, K. (2013) Extremely high-accuracy correction of air refractive index using two-colour optical frequency combs. *Sci. Rep.* 3, 1894 (5 pp.).

Wu, H., Zhao, T., Wang, Z., Zhang, K., Xue, B., Li, J., He, M., and Qu, X. (2017) Long distance measurement up to 1.2 km by electro-optic dual-comb interferometry. Appl. Phys. Lett. 111, 251901 (5 pp.).

Wynands, R., Coste, O., Rembe, C., and Meschede, D. (1995) How accurate is optical second-harmonic generation? *Opt. Lett.* 20, pp. 1095-7.

Yang, R., Pollinger, F., Meiners-Hagen, K., Krystek, M., Tan, J., and Bosse, H. (2015) Absolute distance measurement by dual-comb interferometry with multi-channel digital lock-in phase detection. *Meas. Sci. Technol.* 28, 084001 (10 pp.).